# Intermediate asymptotics on dynamical impact of solid sphere on militextured surface

Hirokazu Maruoka [1,2,*]

[1] *United Graduate School of Agricultural Science, Tokyo University of Agriculture and Technology, 3-5-8 Saiwai-cho, Fuchu-shi, Tokyo 183-8509, Japan*

[2] *Graduate School of Science and Technology, Kwansei Gakuin University, 2-1 Gakuen, Sanda-shi, Hyogo 669-1337, Japan*

(Received 13 June 2019; published 20 November 2019)

Complex phenomena incorporating several physical properties are abundant while they are occasionally revealing the variation of power-law behavior depending on the scale. In the present work, the global scaling behavior of the dynamical impact of a solid sphere onto an elastic surface is described. Its fundamental dimensionless function was successfully obtained by applying dimensional analysis combined with a solution by energy conservation complementally. It demonstrates that its power-law behavior is given by the competition between two power-law relations representing inertial and elastic properties respectively, which is strengthened by the scale size of the sphere. These factors are successfully summarized by the newly defined dimensionless parameters, which give two intermediate asymptotics in a different scale range. These power-law behaviors given by the theoretical model were compared with experimental results, showing good agreement. This study supplies the insights to dimensional analysis and self-similarity in general.

DOI: 10.1103/PhysRevE.100.053004

## I. INTRODUCTION

In the field of the mechanics of continua, including rheology, microfluidics, and fluid mechanics, phenomena incorporating several physical properties are frequently observed. Viscoelasticity exhibits both fluidity and solidity, while a dimensionless number called the Deborah number, $\mathrm{De} = \tau/T$ [1], which is defined as the ratio of relaxation time of materials $\tau$ and observation time $T$, qualifies the property. $\mathrm{De} \ll 1$ qualifies the material as a fluid, while $\mathrm{De} \gg 1$ leads to the qualification as a solid [2]. Here note that dimensionless numbers represent the proportion between properties or forces which govern the phenomena (e.g., the Reynolds number is the ratio between the inertial force and viscous force). In these two cases, the homogeneous physical property can be assumed in each, and the problems generally turn out to be simple. However, the intermediate-scale range reveals characteristic behavior (e.g., viscoelasticity for $\mathrm{De} \sim 1$), in which two physical properties are fundamentally mixed, which turns out to complicated problems that are occasionally difficult to be formalized and conquered even though they are quite attractive and important for the mechanics of continua.

On the other hand, these phenomena can be understood as *intermediate asymptotics* [3,4], which are defined as an asymptotic representation of a function valid in a certain range of independent variables. They are occasionally found as a simple power-law relation through dimensional analysis when some dimensionless parameters are considered to be negligible. More or less all the theories can be considered as intermediate asymptotics, which are valid in a certain scale range [5]. This concept was formalized by Barenblatt [2–4] with the method of dimensional analysis, supplying a universal and coherent view of the physical theory and applications in various areas [6–9]. This methodology is expected to be effective for the complex problems involving plural physical properties though the scale range in which a dimensionless number is extremely large or small is focused. The method is not always applicable and limited to some extent, particularly in the case where problems turn to be self-similar solutions of the second kind. A self-similar solution of the second kind is the problem in which dimensionless parameters have power-law behaviors, and generally these behaviors cannot be clarified within dimensional analysis but occasionally deduced by technical means such as renormalization group theory or a method for nonlinear eigenvalue problems.

The present work focuses on the intermediate-scale range of dimensionless parameters in which several physical properties are incorporated, based on the concept of dimensional analysis and intermediate asymptotics. Here I discuss the relation between dimensionless number and complex behaviors. The problem is the dynamical impact of a solid sphere onto a militextured elastic surface. The dynamical collision is seen in abundant phenomena in our daily lives and is interesting for industry [10] and sports [11,12]. Since Hertz described the collisional dynamics between two elastic bodies [13], the theory was developed as contact mechanics [14]. Recently the collision dynamics between a macrotextured and immersed sphere is studied by Chastel *et al.* [15,16]. A militextured surface can be described by an elastic-foundation model [17], of which the stress profile is simplified.

Chastel *et al.* [15] have already obtained the scaling behavior of dynamical impact of a sphere onto a militextured surface. However, I will show that this scaling behavior is an intermediate asymptotic valid in a certain scale range by applying dimensional analysis. We will recognize the problem belongs to a self-similar solution of the second kind. Finally I attempt to obtain the fundamental dimensionless functions

*maruoka.hirokazu@kwansei.ac.jp; hmaruoka1987@gmail.com

 ©2019 American Physical Society

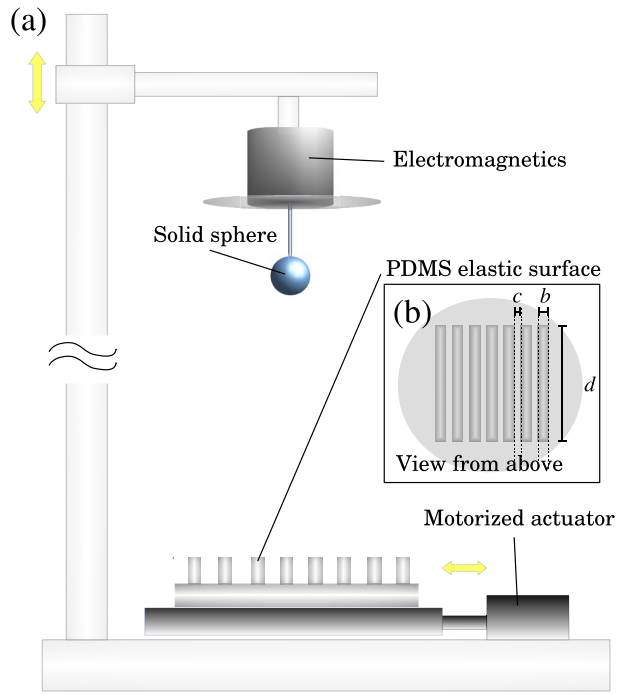


FIG. 1. (a) Sketch of experimental setup. The solid sphere is suspended by an electromagnet which is capable of dropping the ball in arbitrary timing. The velocity of the impact can be adjusted by changing the height of the part in which the sphere is suspended. The position of the elastic surface made of PDMS can be changed with a motorized actuator. (b) View from above the PDMS elastic surface. The striped-pattern rectangular pillars are engraved on the surface.

to describe the global power-law behaviors of this problem by referring to the solution obtained by energy conservation complementally. These theoretical predictions are compared with experimental results to verify the validity of the method.

## II. EXPERIMENT

The experiments have been performed using a militextured surface made of polydimethylsiloxane (PDMS) (Sylvard 180, Dow Corning) as the elastic surface, with elastic modulus $E \simeq 1.6\,\mathrm{MPa}$ (see Fig. 1). The periodic, striped-patterned, rectangular pillars were engraved on the surface, with height of pillar $h = 3.5$ mm, thickness of short sides of pillar $b = 2.5$ mm, length of long side $d = 60$ mm, interdistance of channel $c = 1.5$ mm, and fraction of surface $\phi = bd/(b + c)d = 0.625$ [Fig. 1(b)]. The metallic sphere (Bearing Option Ltd, steel balls) is suspended by an electromagnet (Mecalectro, F91300 Massy, No. 5,18,01) of which the magnetic force is controlled and capable of dropping the sphere in arbitrary timing. The collision impacts were recorded with a high-speed camera (Phantom V7.3) of which the flame rate is 10000 images per second, and its resolution is $512 \times 512$ pixels. The collision velocity is varied by changing the height of position from which the sphere is dropped (1.5–50 cm). The radius of sphere $R$ differs as 3.0, 4.0, 4.5, 5.0, and 7.0 mm, of which density $\rho = 7800\,\mathrm{kg} \times \mathrm{m}^{-3}$. The collision experiments were performed for 30–40 times in each condition, changing the position of the elastic surface every 2.0 mm with a motorized actuator (Standa, 122851) so that the effect of peculiarity between the pillars and sphere was normalized. The information about velocity, deformation, and compression time was extracted from the movies with image analysis using a software programmed using MATLAB.

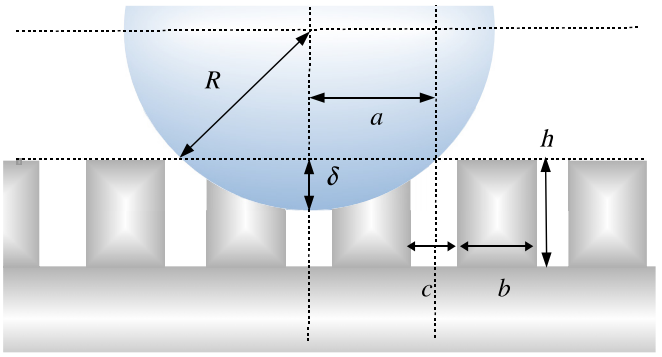


FIG. 2. The geometrical parameters involved in the collision between an elastic surface and solid sphere. Deformation $\delta$ and diameter of contact $a$ are generated by the collision onto the elastic PDMS surface.

## III. THE SCALING RELATION: THE RESULT BY CHASTEL *et al.*

First, I show the scaling solutions of this problem obtained by Chastel *et al.* [15].

The collision of a sphere falling with a velocity of $v$ onto the surface generating the parabolic deformation $\delta$ is sketched in Fig. 2. In small deformation, the parabolic deformation is due to the geometrical relation, and thus it is described as $\delta(r) = \delta[1 - (r/a)^2]$. According to the theory of Hertz, the contact radius $a$ is important parameter, which is obtained geometrically, $a^2 = R^2 - (R - \delta)^2 \simeq 2R\delta$, as well. First, the kinetic energy of the sphere is easily obtained as

$$E_{ki} = \frac{2}{3}\pi R^3 \rho v^2. \tag{1}$$

Following the procedure of Chastel *et al.* [15], as the normal stress is $\sigma(r) = E\delta(r)/h$, the force of deformation is $F = \int_0^a \phi\sigma(r) 2\pi r\, dr = \pi E\phi R\delta^2/h$ by eliminating $a$ by $a^2 = 2R\delta$. Thus the elastic energy is obtained as

$$E_{el} = \int_0^\delta F(\delta')\, d\delta' = \frac{\pi E\phi\delta^3 R}{3h}. \tag{2}$$

Thus the conservation equation for kinetic energy and elastic energy at instant $t$ after the collision are described as follows:

$$\frac{2}{3}\pi R^3\rho v(t)^2 + \frac{\pi E\phi R\delta(t)^3}{3h} = \frac{2}{3}\pi R^3\rho v_i^2. \tag{3}$$

where $v_i$ is the initial velocity in which the sphere touches the surface. The maximum penetration $\delta_{m0}$ is reached when $v(t) = 0$, and then the following relation is obtained:

$$\frac{\delta_{m0}}{R} = \left(\frac{2}{\phi}\right)^{\frac{1}{3}} \left(\frac{h}{R}\right)^{\frac{1}{3}} \left(\frac{\rho v_i^2}{E}\right)^{\frac{1}{3}}. \tag{4}$$

Compression time $\tau_c$, which is defined as the duration time at which the sphere contacts with the surface [18], is obtained

as follows:

$$\tau_c = 2\,\frac{\delta_{m0}}{v_i}\int_0^1 \frac{d(\delta'/\delta)}{\sqrt{1-(\delta'/\delta)^3}} = \frac{2}{3}B\left(\frac{1}{3},\frac{1}{2}\right)\frac{\delta_{m0}}{v_i}, \quad (5)$$

where $B(x, y)$ is a beta function. Thus following equation is obtained from Eq. (4):

$$\frac{\tau_c v_i}{R} = \frac{C_0}{\phi^{\frac{1}{3}}}\left(\frac{h}{R}\right)^{\frac{1}{3}}\left(\frac{\rho v_i^2}{E}\right)^{\frac{1}{3}}, \quad (6)$$

where $C_0 = 2\sqrt[3]{2}/3\,B(\frac{1}{3},\frac{1}{2}) \simeq 3.533$.

These are the results of Chastel *et al.* [15]. However, next I show that these scaling relations are intermediate asymptotics which are valid in a certain range.

## IV. DIMENSIONAL ANALYSIS: SCALING BETWEEN Π and η

Based on the recipe of Barenblatt [19], first, the function to study $\delta_{m0} = f(a, R, \rho, E, v_i, h, \phi)$ is proposed. Assuming a $LMT$ unit, the dimensionless parameters are constructed. Here I selected $R, \rho, v_i$ as the governing parameters with independent dimensions, which are the parameters which cannot be represented as a product of the remaining parameters. As $\delta_{m0} = L$, $R = L$, $a = L$, $\rho = M/L^3$, $E = M/LT^2$, $v_i = L/T$, $h = L$, $\phi = 1$, the following dimensionless parameters are obtained:

$$\Pi = \frac{\delta_{m0}}{R}, \quad \xi = \frac{a}{R}, \quad \eta = \frac{\rho v_i^2}{E}, \quad \kappa = \frac{h}{R}. \quad (7)$$

Thus the function is transformed to $\Pi = \Phi(\xi, \eta, \kappa, \phi)$, where $\Phi$ is an arbitrary dimensionless function. Here let us assume that the problem belongs to the self-similar solutions of the second kind [20] as follows:

$$\Pi = \phi^{\gamma_1}\kappa^{\gamma_2}\eta^{\gamma_3}\Phi(\xi^{\zeta_1}\kappa^{\zeta_2}\phi^{\zeta_3}\eta^{\zeta_4}). \quad (8)$$

Self-similar solutions of the second kind are the dimensional analysis solutions, which are expressed by the products of dimensionless parameters raised to the powers, though the power exponents of dimensionless parameters are not obtained within dimensional analysis in principle. However, in our case, power exponents $\gamma_1 \cdots \gamma_3$ can be deduced via Eq. (4). $\zeta_1 \cdots \zeta_4$ are obtained by utilizing Eq. (4) and $a^2 = 2R\delta$, and then it is $\xi \sim \phi^{-1/6}\kappa^{1/6}\eta^{1/6}$. Therefore Eq. (8) leads to

$$\Pi = \left(\frac{\kappa}{\phi}\right)^{\frac{1}{3}}\eta^{\frac{1}{3}}\Phi\left[\left(\frac{\phi}{\kappa}\right)^{\frac{1}{6}}\xi/\eta^{\frac{1}{6}}\right]. \quad (9)$$

Equation (9) is the fundamental dimensionless function which describes the dynamical impact of the solid sphere on the militextured surface. Supposing new parameters $\Psi = \Pi\phi^{1/3}\kappa^{-1/3}\eta^{-1/3}$ and $\Xi = \xi\phi^{1/6}\kappa^{-1/6}\eta^{-1/6}$, Eq. (9) is described as $\Psi = \Phi(\Xi)$. Note that $\Psi$ is a function with dimensionless parameter $\Xi$. It suggests that the scaling relation derived from the result by Chastel *et al.* [15] is confirmed as long as $\Phi$ does not interfere. In this case the following intermediate asymptotic is obtained:

$$\Pi = \text{const}\left(\frac{\kappa}{\phi}\right)^{\frac{1}{3}}\eta^{\frac{1}{3}}, \quad (10)$$

which corresponds to Eq. (4). This condition holds true in the case that $\Xi$ is small enough to consider $\Phi \sim$ const. Here we have recognized that $\Xi$ is an important parameter dominating the power-law behavior.

Next, let us move on to the case in which $\Xi$ contributes to the behavior. It is quite interesting to think what kind of intermediate asymptotic is obtained in another scale region. Equation (9) was obtained by the dimensionless parameters via the selection of governing parameters with independent dimensions as $R, \rho, v_i$. However, this choice is arbitrary. Barenblatt [19] suggested that the numerical estimation of dimensionless parameters can help us to choose. If the dimensionless parameters to consider are too small or large, these dimensionless parameters can be considered to be negligible. The choice of $R, \rho, v_i$ is appropriate in the case in which these three parameters play a dominant role. However, the scale range in which $\Xi$ contributes must have $a$ large enough to be considered as $\xi = a/R$ increases $\Xi$. In this case, $a$ should be considered as a dominant parameter.

Now let us apply the dimensional analysis using another selection of governing parameters with independent dimensions as $a, \rho, v_i$. In this case the following dimensionless parameters are finally obtained:

$$\Pi' = \frac{\delta_{m0}}{a}, \quad \xi = \frac{a}{R}, \quad \eta = \frac{\rho v_i^2}{E}, \quad \kappa' = \frac{h}{a}. \quad (11)$$

The difference from Eq. (7) is that $\Pi$ and $\kappa$ are replaced by $\Pi'$ and $\kappa'$ while $\Pi = \xi\Pi'$ and $\kappa = \xi\kappa'$. Similarly, assuming self-similarity of the second kind and using Eq. (4) and $a^2 \sim R\delta$, the following intermediate asymptotic is obtained in another scale region:

$$\Pi' = \text{const}\left(\frac{\xi\kappa'\eta}{\phi}\right)^{\frac{1}{6}}. \quad (12)$$

Equation (12) is another intermediate asymptotic in the case where $a$ is comparatively large enough.

The following calculation will justify our interpretation. In order to see the behavior of Eq. (9) in a wider scale region from small $\Xi$, series expansion of $\Phi$ in a power of $\Xi$ is applied as follows:

$$\begin{aligned}\Pi &= \left(\frac{\kappa}{\phi}\right)^{\frac{1}{3}}\eta^{\frac{1}{3}}\{A_1 + A_2\,\Xi + A_3\,\Xi^2 + \cdots\} \\ &= A_1\left(\frac{\kappa}{\phi}\right)^{\frac{1}{3}}\eta^{\frac{1}{3}} + A_2\,\xi\left(\frac{\kappa}{\phi}\right)^{\frac{1}{6}}\eta^{\frac{1}{6}} + A_3\,\xi^2 + \cdots, \end{aligned} \quad (13)$$

where $A_1, A_2, A_3$ are constants. Here let us focus on the fact that two dimensionless parameters having different power exponents appear in Eq. (13). Suppose one fits Eq. (13) with an arbitrary power equation of $\eta$ as $\eta^\nu \sim A_1\,\phi^{-1/3}\kappa^{1/3}\eta^{1/3} + A_2\,\xi\phi^{-1/6}\kappa^{1/6}\eta^{1/6} + A_3\xi^2$, the power exponent $\nu$ is *locally* determined and varies in the range $1/6 \leqslant \nu \leqslant 1/3$, depending on the contribution of the first term and second term in Eq. (13). This balance critically depends on parameter $\eta$ and $\xi$. We can see that in case of small $\eta$ and large $\xi$, the power exponent of the second term $1/6$ is dominant. On the other hand, in the case of large $\eta$ with small $\xi$, the first term is large and dominant, then $\nu$ should be fitted with $1/3$. This interpretation corresponds to each intermediate asymptotics [Eq. (10)

and Eq. (12)] as small $\Xi$ indicates that the contribution of the second term is extremely small.

This is spontaneously understood as $\Xi$ is given by ratio of the first and second terms as $\xi\phi^{-1/6}\kappa^{1/6}\eta^{1/6}/\phi^{-1/3}\kappa^{1/3}\eta^{1/3} = \xi\phi^{1/6}\kappa^{-1/6}\eta^{-1/6} = \Xi$. In the end, series expansion of $\Phi(\Xi)$ gives two intermediate asymptotics which are obtained by different selection of governing parameters with independent dimensions, and $\Xi$ represents the ratio between two intermediate asymptotics.

## V. DIMENSIONAL ANALYSIS: SCALING BETWEEN $\omega$ and $\eta$

Next let us apply the same way to construct the dimensionless function concerning Eq. (5). The function to study is $\tau_c = f_\tau(a, R, \rho, E, v_i, h, \phi)$. Assuming the governing parameters with independent dimensions as $R$, $\rho$, $v_i$, the following dimensionless parameters are to be prepared:

$$\omega = \frac{\tau_c v_i}{R}, \quad \xi = \frac{a}{R}, \quad \eta = \frac{\rho v_i^2}{E}, \quad \kappa = \frac{h}{R} \tag{14}$$

to obtain $\omega = \Phi_\tau(\xi, \eta, \kappa, \phi)$. Here we assume the self-similar solution of second kind, and we find the fundamental dimensionless function

$$\omega = \left(\frac{\kappa}{\phi}\right)^{\frac{1}{3}} \eta^{\frac{1}{3}} \Phi_\tau\left[\left(\frac{\phi}{\kappa}\right)^{\frac{1}{6}} \xi/\eta^{\frac{1}{6}}\right] \tag{15}$$

by referring to Eq. (5) and $a^2 = 2\delta R$. Defining $\Omega = \omega\phi^{1/3}\kappa^{-1/3}\eta^{-1/3}$, here we find the relation as $\Omega = \Phi_\tau(\Xi)$, suggesting the dependence between $\Omega$ and $\Xi$. Equation (15) gives an intermediate asymptotic corresponding to Eq. (5) as far as $\Xi$ is uninfluential, then we have $\omega \sim \eta^{1/3}$. However, in the scale range in which $a$ starts to play a role and $\Xi$ is large enough, another intermediate asymptotic appears,

$$\omega = \text{const}\,\xi\left(\frac{\kappa}{\phi}\right)^{\frac{1}{6}} \eta^{\frac{1}{6}}, \tag{16}$$

which is obtained by the series expansion of $\Phi_\tau$ as the second term, or corresponds to the solution obtained through the dimensional analysis by the selection of the governing parameters with independent dimensions as $a$, $\rho$, $v_i$. In this case, the scaling relation $\omega \sim \eta^{1/6}$ appears.

## VI. COMPARISON WITH EXPERIMENTAL RESULTS

Once the sphere is released from the electromagnetic force, it starts to free fall and collides with the PDMS surface to generate the maximum deformation from 0.87–2.8 mm, depending on the size of sphere and height from which the ball drops [see Figs. 3(a)–3(c) and the Supplemental Material for the movie [21]]. The number of rectangular pillars contacted by the sphere also depends on the size. The smallest sphere ($R = 3.0$ mm) contacted 1–2 pillars, while the middle spheres ($R = 4.0$, 4.5 mm) contacted generally two pillars, and the larger sphere ($R = 5.0$, 7.0 mm) contacted 2–3 pillars. However, the difference of the number of pillars is normalized as the experiments of one fixed condition (height, size of sphere) are performed for 30–40 times, while the position of PDMS surface changed by the equipped actuator for 2.0 mm on every

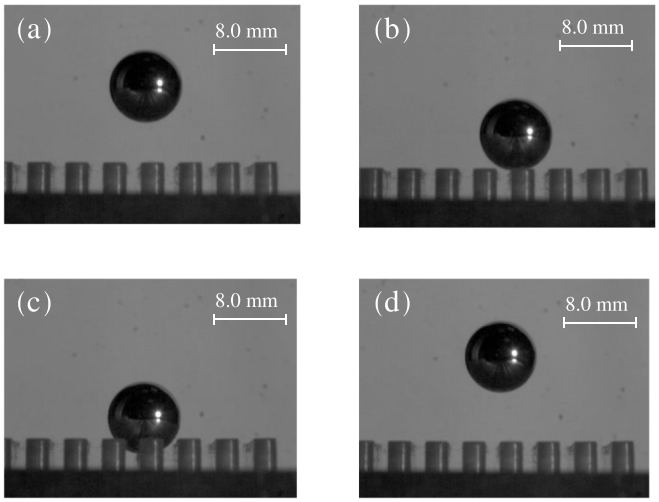


FIG. 3. The images of the dynamical impact of sphere ($R = 4.0$ mm) onto the elastic surface at $v_i = 2.4$ m/s with a flame rate of 10000 images per second and a resolution of $512 \times 512$ pixels. (a) The image before impact. (b) The moment of contact. (c) The moment of maximum deformation at $t = 10$ ms after contact. (d) The image releasing from surface at $t = 60$ ms after contact. The movie is available in the Supplemental Material [21].

impact. The deformations and contact times are estimated by averaging these results. After a certain compression time $\tau_c$ (2.0–6.0 ms), it takes off out of the surface [Fig. 3(d)].

In order to compare with the theoretical prediction, numerical results were nondimensionalized following defined dimensionless parameters, $\Pi$, $\eta$, $\xi$, and $\kappa$. Figure 4(a) is the plots of $\Pi$ and $\eta$ with different sizes of sphere. It is clearly found that the power-law behavior varies depending on the size of sphere. The largest sphere $R = 7.0$ mm follows the 1/3 power-law behavior, corresponding to Eq. (10). On the other hand, the smallest spheres $R = 3.0$ mm reveal different power-law behavior, following the 1/6 power law, which corresponds to Eq. (12).

Figure 4(b) is the plots of $\Psi = \Phi(\Xi)$ using experimental data. It is useful to see in which scale range each plot belongs. We can see that plots of the small sphere ($R = 3.0$ mm), which follows a 1/6 power law, belong to larger $\Xi$, while the plots with high velocity decrease $\Xi$. Contrarily it is found that the large sphere ($R = 7.0$ mm) belongs to smaller $\Xi$, though plots with small velocity belong to comparatively larger $\Xi$, which reveals different behavior. Meanwhile, we can find the groups of intermediate size of sphere ($R = 4.0$, 4.5, 5.0 mm), which belong to $\Xi = 1.1$–1.4, follow intermediate power-law behaviors. It can be considered that these plots belong to an intermediate-scale region in which two power exponents are competing.

The different power-law behavior depending on size of the sphere can be seen in the plots of $\omega$ and $\eta$ as well [Fig. 5(a)]. The dimensional analysis predicted two power-law behaviors, $\omega \sim \eta^{1/3}$ at small $\Xi$ and $\omega \sim \eta^{1/6}$ at large $\Xi$. The plots of the largest sphere ($R = 7$ mm), having small $\Xi$ as is shown in Fig. 5(b), follows 1/3 power-law behavior which corresponds to Eq. (6). The plots of the smallest sphere ($R = 3$ mm) reveal mixed behavior, though the plots having smaller $\eta$, belonging

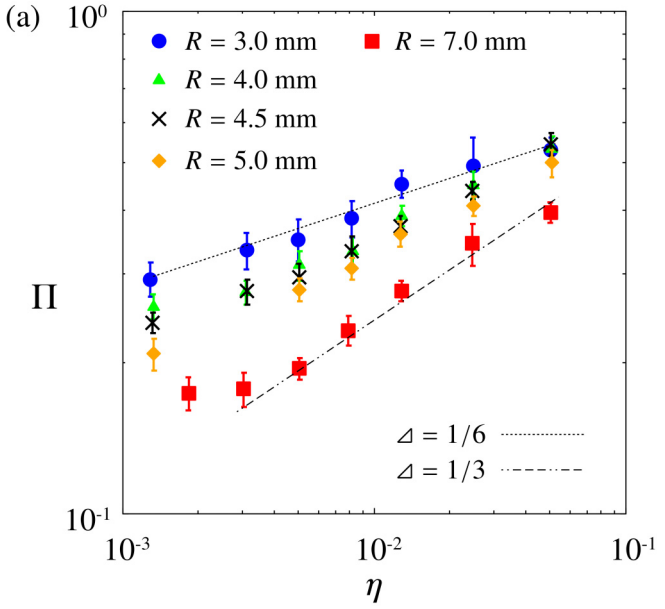


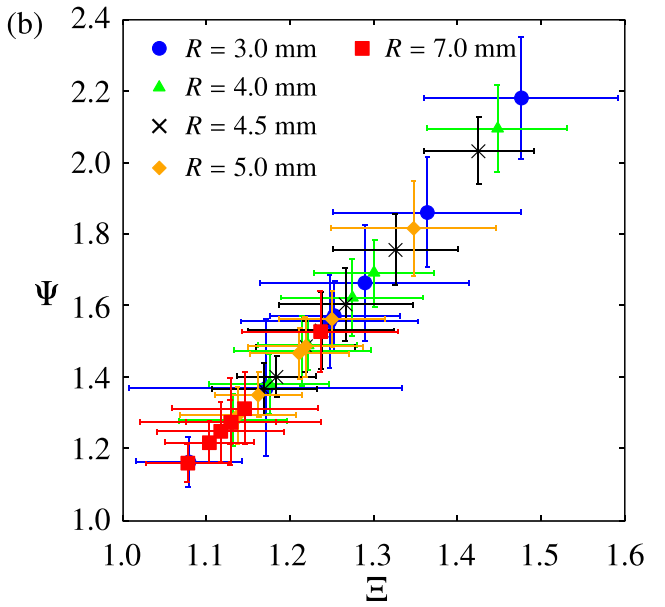


FIG. 4. (a) Power-law relation between $\Pi$ and $\eta$, (b) plots of $\Psi$ vs $\Xi$ with different sizes of the sphere, $R = 3.0$ mm (●), 4.0 mm (▲), 4.5 mm (×), 5.0 mm (◆), and 7.0 mm (■), where $\Pi = \delta_{m0}/R$, $\eta = \rho v_i/E$, $\Psi = \Pi\phi^{1/3}\kappa^{-1/3}\eta^{-1/3}$, and $\Xi = \xi\phi^{1/6}\kappa^{-1/6}\eta^{-1/6}$. The two dashed lines indicate the slope of 1/6 and 1/3.

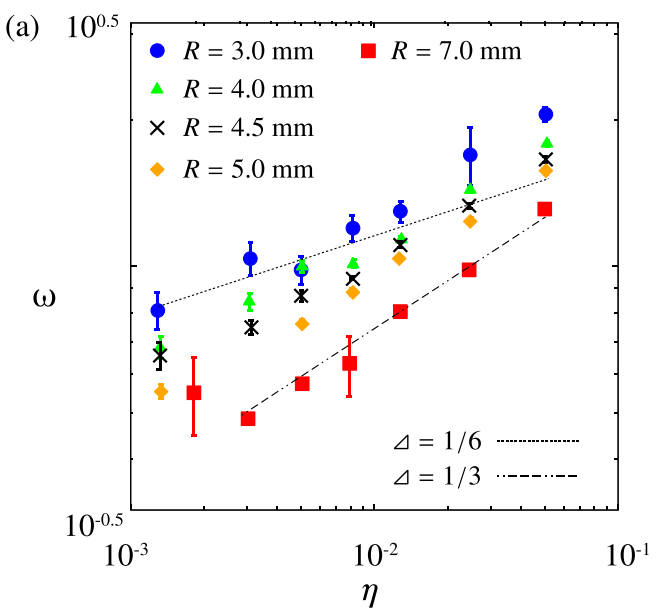


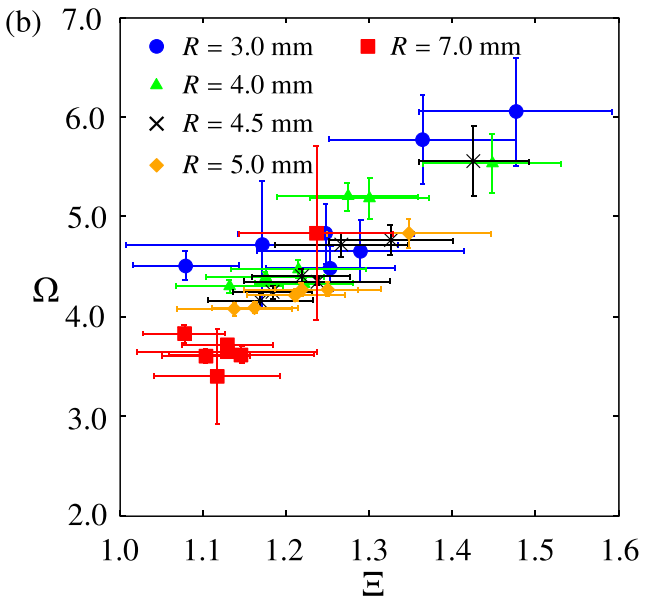


FIG. 5. (a) Power-law relation between $\omega$ and $\eta$, (b) plots of $\Omega$ vs $\Xi$ with different sizes of the sphere, $R = 3.0$ mm (●), 4.0 mm (▲), 4.5 mm (×), 5.0 mm (◆), 7.0 mm (■), where $\omega = \tau_c v_i/R$, $\eta = \rho v_i/E$, $\Omega = \omega\phi^{1/3}\kappa^{-1/3}\eta^{-1/3}$ and $\Xi = \xi\phi^{1/6}\kappa^{-1/6}\eta^{-1/6}$. The two dashed lines indicate the slope of 1/6 and 1/3.

to large $\Xi$ in Fig. 5(b), follow a 1/6 power-law behavior of Eq. (16). The plots of the intermediate size sphere follow intermediate behavior. Focusing on $\Xi$ in detail, we can find that it consists of $\phi$, $\kappa$, $\xi$ and $\eta$. $\phi$ and $\kappa$ are dimensionless parameters which belong to elastic surface; here we focus on the others. $\eta$, which corresponds to the Cauchy number, which is defined as the ratio of inertial force and elastic force in fluid mechanics, plays a dominant role on the impact. This parameter reflects the degree of contribution derived from elasticity and inertia. Therefore I would like to call the impact following the 1/6 power law the elasticity-dominant impact, and the one following the 1/3 power law the inertia-dominant impact [22].

Not only $\eta$ but also $\xi$ is a key parameter. The second term of Eq. (13), which corresponds to the intermediate asymptotic of the elasticity-dominant impact, is multiplied by $\xi$, indicating that the contribution of the second term is critically weakened by small $\xi$. $\xi$ measures the relative degree of subsidence into the surface. A smaller sphere subsides relatively deeper than larger one (Fig. 6), which is the reason why the small sphere ($R = 3.0$ mm) follows a 1/6 power behavior. In the end, this physical interpretation of $\Xi$ corresponds to the analytical interpretation of Eq. (13), which proves the validity of the application of dimensional analysis.

Ledesma-Alonso *et al.* discussed the elastic contact between a spherical lens and a patterned surface [23], showing

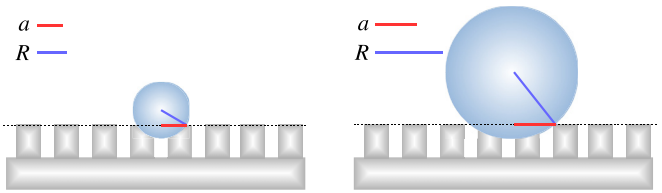


FIG. 6. Comparison of wall-sphere contact generating geometrical dimensionless parameter $\xi = a/R$ in a smaller (left) and larger value (right).

that the indentation behavior is changed depending on the fraction $\phi$. $\phi$ may differ locally in the smaller sphere because the smallest one ($R = 3.0$ mm) is not quite larger than the thickness of the rectangular pillar ($b = 2.5$ mm, $c = 1.5$ mm). However, these effects are normalized by collecting the data, while the position of elastic surface is slightly (2.0 mm) changed on every impact for every condition. Furthermore, $\phi$ is also related to power-law behavior in our case as $\phi$ is included in $\Xi$. As Fig. 4(a) shows, a plot of $R = 7.0$ mm which belongs to larger $\Xi$ shows different behavior even if its size is equal. It suggests that fundamental behavior is decided by $\Xi$, not by single dimensionless parameters.

As periodic, striped-pattern pillars are inscribed, each pillar is independent against deformation. Thus, each pillar is mainly deformed in a vertical line even in the impact of a small sphere, in which the contact radius $a$ can be smaller than the surface of the rectangular pillar $b$. It signifies that the present model, the elastic foundation model, in which the stress profile is simplified for normal stress, is still valid for the impact of the small sphere.

These new intermediate asymptotics [Eq. (12) and Eq. (16)] are obtained in the course of dimensional analysis, not in an analytical manner. Not all the solutions obtained by dimensional analysis are solved analytically either, as this method is developed and applied for the problems in which the analytical treatment is difficult. However, Eq. (9) is obtained naturally by following Chastel's solution with assumption of a self-similar solution of the second kind, and that it gives the solution from series expansion in Eq. (13). These theoretical results are consistent with the experimental results and physical interpretation that the power-law behavior is decided by the competition between elasticity and inertia. This consistency justifies the conclusion though analytical expression can remain a problem.

In other reports of contact mechanics, the property of deformation is changed from elastic contact to plastic contact giving different power laws, depending on the scale of interference [24]. The high-speed impact generates the plastic deformation depending on the dimensional parameters [25]. The present work discovered another scale-dependent phenomenon of contact mechanics. The scale dependence of power-law behavior is occasionally observed in self-similarity of the second kind [26,27], while the dependence is sometimes semiempirical [28]. This work clearly identified the dependence of the dimensionless parameter as the competition between two power exponents.

## VII. CONCLUSION

In conclusion, the above discussion with experimental results confirms the validity of Eq. (9) and Eq. (15) as the fundamental dimensionless functions of this problem. Equation (9) and Eq. (15) include the information of *global* scaling behaviors, which give two intermediate asymptotics *locally*, depending on $\Xi$. This *scale locality* was quite important for understanding this phenomenon as even the power-law behavior depended on the scale.

The present work is unique on the point that the intermediate-scale range in which two physical properties are incorporated is focused upon, and the crossover of power-law behaviors is explained as the result of competition between two intermediate asymptotics each representing different physical properties. Generally, the cases in which the uniformity of a physical property can be assumed tend to be concentrated, while the intermediate region is avoided. However, this work dealt with this intermediate region, and the crossover of power-law behavior was confirmed with experimental results. Furthermore, the two different methods were combined complementally in this work: dimensional analysis and the solution obtained by the equation of kinetic energy and elastic energy. Generally the latter solution is considered to be enough, but the scale dependence would not have been recognized without dimensional analysis. This suggests that this combined dimensional analysis with the concept of an intermediate asymptotic is quite effective to analyze the mesoscale phenomena incorporating two or more physical properties, revealing different behaviors depending on the scale.

In this work, self-similarity of the second kind is understood as the competition between two intermediate asymptotics. This is also a quite interesting insight for the concept of self-similarity in general.

## ACKNOWLEDGMENTS

The author wishes to thank J.-B. Besnard, P. Panizza, and L. Courbin for technical assistance with the experiments. He thanks K. Osaki for theoretical advice. This work was supported by the program Long-Term Internship Dispatch for Innovation Leader Training organized by the Building of a Consortium for the Development of Human Resources in Science and Technology.

[1] M. Reiner, The Deborah number, Phys. Today **17**(1), 62 (1964).
[2] G. I. Barenblatt, *Flow, Deformation and Fracture* (Cambridge University Press, Cambridge, 2014), p. 3.
[3] G. I. Barenblatt and Ya. B. Zeldovich, Self-similar solutions as intermediate asymptotics, Annu. Rev. Fluid Mech. **4**, 285 (1972).
[4] G. I. Barenblatt, *Scaling* (Cambridge University Press, Cambridge, 2003).
[5] The forward of Ref. [2], by A. J. Chorin, is quite suggestive, in which he says, "Most physical theories are intermediate, in the sense that they describe the behavior of physical systems on spatial and temporal scales intermediate between much smaller

scales and much larger scales; for example, the Navier-Stokes equations describe fluid motion on spatial scale larger than molecular scales but not so large that relativity must be taken into account and on time scales larger than the time scale of molecular collisions but not so large that the vessel that contains the fluid collapses through aging." For example, the ideal gas equation can be considered as an intermediate asymptotic valid in the range where the volume of molecules $b$ and the molecular interaction $a$ are negligible on a van der Waals equation as follows:

$$p = \frac{nRT}{V - nb} - \frac{an^2}{V^2} \longrightarrow \frac{nRT}{V}\left(\frac{an^2}{V^2} \ll p \ll \frac{RT}{b}\right).$$


[6] L. Banetta and A. Zaccone, Radial distribution function of Lennard-Jones fluids in shear flows from intermediate asymptotics, Phys. Rev. E **99**, 052606 (2019).

[7] S. Boscolo and S. K. Turitsyn, Intermediate asymptotics in nonlinear optical systems, Phys. Rev. A **85**, 043811 (2012).

[8] N. Goldenfeld, O. Martin, and Y. Oono, Intermediate asymptotics and renormalization group theory, J. Sci. Comput. **4**, 355 (1989).

[9] G. I. Barenblatt and A. J. Chorin, A mathematical model for the scaling turbulence, Proc. Natl. Acad. Sci. USA **101**, 15023 (2004).

[10] I. G. Goryacheva, *Contact Mechanics in Tribology* (Kluwer Academic Publishers, Dordrecht, 1998).

[11] R. W. Carpick, Approximate models of interacting surfaces competed against a supercomputer solution, Science **359**, 38 (2018).

[12] A. M. Nathan, J. J. Crisco, R. M. Greenwald, D. A. Russell, and L. V. Smith, A comparative study of baseball bat performance, Sports Eng. **13**, 153 (2011).

[13] H. Hertz, *Miscellaneous Papers* (Macmillan, London, 1896), p. 146.

[14] K. L. Johnson, *Contact Mechanics* (Cambridge University Press, Cambridge, 1985).

[15] T. Chastel, P. Gondret, and A. Mongruel, Texture-driven elastohydrodynamic bouncing, J. Fluid Mech. **805**, 577 (2016).

[16] T. Chastel and A. Mongruel, Sticking collision between a sphere and a textured wall in a viscous fluid, Phys. Rev. Fluids **4**, 014301 (2019).

[17] See Ref. [14], p. 104.

[18] See Refs. [14] (p. 353) and [15].

[19] See Ref. [4] (pp. 91–93).

[20] According to the category by Barenblatt [see Ref. [3], [4] (pp. 87–89), or [2] (pp. 153–163)], *self-similar solutions of the first kind* or *complete similarity* are the solutions which possess the invariance against scale transformation, which can be described as $\Pi = \Phi(\Pi_1, \Pi_2, \Pi_3)$ where $\Pi \cdots \Pi_3$ are dimensionless parameters. By contrast, *self-similar solutions of the second kind* or *incomplete similarity* are the solutions that no longer have scale invariance and possess the power-law-form such as $\Pi = \Pi_2^{\alpha}\Phi(\Pi_1/\Pi_2^{\beta}, \Pi_3)$ of which $\alpha$, $\beta$ cannot be obtained by only dimensional analysis in principle.

[21] See Supplemental Material at http://link.aps.org/supplemental/10.1103/PhysRevE.100.053004 for a dynamical impact of sphere ($R = 4.0$mm) onto the elastic surface at $v_i = 2.4$m/s with a flame rate of 10000 images per second and a resolution of $512 \times 512$ pixels.

[22] Simply calling something an elastic impact or inertial impact may create confuse with the term *elastic impact*, which has already been defined as the collision of which the coefficient of restitution equals 1.

[23] R. Ledesma-Alonso, E. Raphaël, L. Léger, F. Restagno, and C. Poulard, Stress concentration in periodically rough Hertzian contact: Hertz to soft-flat-punch transition, Proc. R. Soc. A. **472**, 20160235 (2016).

[24] L. Kogut and I. Etsion, Elastic-plastic contact analysis of a sphere and a rigid flat, J. Appl. Mech. **69**, 657 (2002).

[25] W. Johnson, *Impact Strength of Materials* (Edward Arnold, London, 1972]); also, e.g., see Ref. [14] (p. 366).

[26] G. I. Barenblatt, A. J. Chorin, and V. M. Prostokishin, A model of a turbulent boundary layer with a nonzero pressure gradient, Proc. Natl. Acad. Sci. USA **99**, 5572 (2002).

[27] G. C. Berry and T. G. Fox, The viscosity of polymers and their concentrated solutions, Adv. Polym. Sci. **5**, 261 (1968).

[28] G. I. Barenblatt and L. R. Botvina, Incomplete similarity of fatigue in a linear range of crack growth, Fatigue Eng. Mater. Struct. **3**, 193 (1981).